Europhys. Lett., 22 (3), pp. 175-180 (1993)

Transition to Filamentary Regime in Laser-Plasma Interaction Evidenced by 2ω Emission.

V. BIANCALANA (*), M. BORGHESI (*), P. CHESSA (*), I. DEHA (**), A. GIULIETTI (*), D. GIULIETTI (***)L. A. GIZZI (*$_*$*) and O. WILLI (*$_*$*)

(*) *Istituto di Fisica Atomica e Molecolare - Via del Giardino 7, 56127 Pisa, Italy*
(**) *Université Boumedienne - Algiers, Algeria*
(***) *Dipartimento di Fisica, Università di Pisa - Pisa, Italy*
(*$_*$*) *Blackett Laboratory, Imperial College - London, UK*

(received 9 November 1992; accepted in final form 1 March 1993)

PACS. 52.35M – Nonlinear waves and nonlinear interactions.
PACS. 52.40D – Electromagnetic wave propagation in plasma.

Abstract. – The level of second-harmonic light emitted from a laser-exploded foil plasma at nominal irradiance up to $3 \cdot 10^{13}$ W/cm^2 was found to be extremely sensitive to both target position and irradiance on target. Either a small target displacement or a small increase in irradiance resulted in a jump of the 2ω level of more than three orders of magnitude. Correspondingly, a transition was observed from a 2ω source pattern clearly signed by the original laser spot pattern to unstable patterns of filaments whose size is consistent with the maximum growth of the instability.

Filamentation is still a puzzling phenomenon at the frontiers of laser plasma research [1]. Its suppression is a relevant step to laser fusion and a field of research is devoted to study the effect of different beam-smoothing techniques on filamentation and related non-linear effects. Recently, very encouraging results have been obtained in long-scalelength plasma experiments [2], even though whole-beam self-focusing seems to remain active also after smoothing [3]. Several diagnostics have been developed so far in order to both understand the physics of this instability and control its effects on laser-plasma interaction [4-6]. The second harmonic generated in filaments is among the possible diagnostics for the instability because it originates from density and field gradients in underdense plasmas [7]. Observations of second-harmonic emission in the presence of filamentary structures have been reported both from solid-target plasmas and gases [8]. In a recent experiment [9], a filamentary perturbation was artificially induced in a plasma in order to find where the second harmonic was actually generated. From the spectroscopic point of view, an interesting result [10] was obtained on the second harmonic emitted sidewards from laser-irradiated exploding-foil plasmas. Time-resolved spectra showed that the second harmonic was red-shifted consistently with frequency sum of laser light with Brillouin back-scattered light.

Simple measurements of conversion efficiency to second-harmonic light do not allow

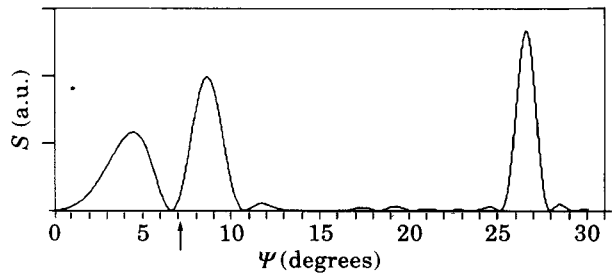

Fig. 1. – The amplitude S of the Poynting vector integrated over the polar angle is reported as a function of the azimuthal angle Ψ. A 50 μm filament with 4 μm radius and $n_c/4$ density was considered. A lower density would increase the light collected by our optics whose aperture angle is marked with the arrow.

already existing plasma gradients and beam non-uniformities to be discriminated from gradients generated by filamentation processes. Experimental data reported so far are often ambiguous in this respect. Our measurements indicate a clear transition to filamentary regime with a threshold intensity dramatically depending on the focusing geometry. The level of forward-emitted second harmonic was considerably higher than sidewards and it was possible to obtain 2D time-resolved images of the 2ω sources in the cross-section of the interaction region. The detection geometry is similar to that used in a previous experiment in gas [8, 11]. The leading role in the harmonic generation is played by gradients perpendicular to the laser beam axis. In fact, with suitable assumptions [8], the 2ω current density is expected to fulfil the equation [1]

$$\boldsymbol{J}_{2\omega} = \frac{ie^3}{m_e^2\omega^3}\left[\frac{n_e}{4}\nabla(\boldsymbol{E}_\omega\cdot\boldsymbol{E}_\omega) + \frac{(\nabla n_e\cdot\boldsymbol{E}_\omega)\boldsymbol{E}_\omega}{1-\dfrac{\omega_p^2}{\omega^2}}\right],$$

where e, m_e and n_e are the electron charge, mass and density, respectively, $\boldsymbol{E}_\omega$ the electric field at the laser frequency ω, and ω_p the electron plasma frequency. As is apparent, the bulk of a uniform plasma cannot generate a second harmonic. If we assume that gradients are related to filaments of length L and radius r, we can write the Poynting vector, far from the filaments, in the form

$$\boldsymbol{S} = A\frac{L^2}{R^2\omega^4}E_\omega^4 n_e^2 r^2 \frac{\boldsymbol{R}}{R}\frac{\sin^2(\chi)}{\chi^2}f(\psi),$$

where A depends only on universal constants, $\boldsymbol{R}$ is the vector from the filament to the observer. The formula is integrated over the polar angle with respect to the filament axis. ψ is the azimuthal angle. The Poynting vector is a function of $\chi = (L/2)(2k_\omega - k_{2\omega}\cos\psi)$, where k_ω and $k_{2\omega}$ are the wave vectors of the fundamental and second-harmonic light, respectively. The functions $f(\psi)$ and $\sin^2\chi/\chi^2$ modulate each other. $\sin^2\chi/\chi^2$ has its main peak where $\cos\psi = 2k_\omega/k_{2\omega}$, while $f(\psi)$ has several maxima close to $\psi = 0$ but vanishes at $\psi = 0$. In fig. 1 a plot is reported of the function $S(\Psi)$ calculated at values of plasma parameters which are typical of our plasma conditions.

The beam-target configuration was the same as in a previous experiment [10]. A plastic (formvar) thin foil was irradiated at 1064 nm laser wavelength with a pulse of 3 ns FWHM at

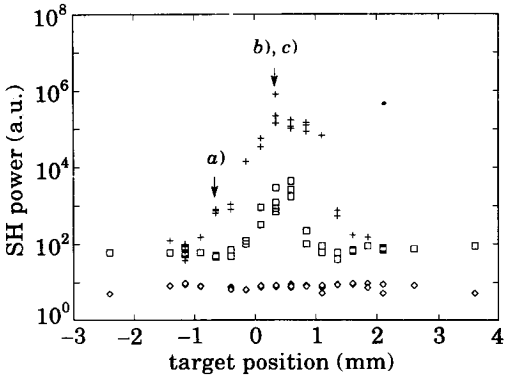

Fig. 2

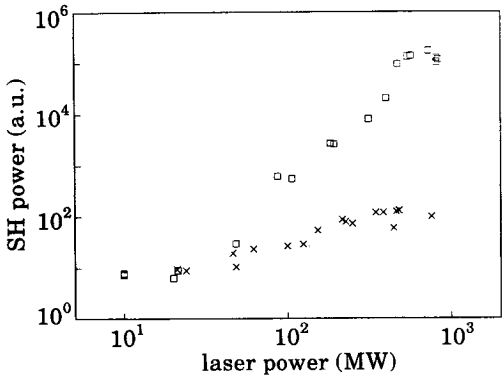

Fig. 3

Fig. 2. – Forward second-harmonic power as a function of target position along the beam axis. Zero position corresponds to target at the nominal best focus. Values of abscissa increase with target distance from the focusing lens. Data obtained at three different laser powers are reported: $\diamond$ P_L = = 15 MW, $\square$ P_L = 170 MW, + P_L = 800 MW. Target thickness was 1 μm. Arrows indicate the two target positions at which 2ω images of fig. 4*a*), *b*) and *c*), respectively, were taken.

Fig. 3. – Forward second-harmonic power as a function of irradiance for a 1 μm target at the position of maximum emission and at − 1.15 mm far from the best focus (× target position = − 1150 μm, □ target position = + 600 μm).

an irradiance up to $3 \cdot 10^{13}$ W/cm^2. The laser beam was focused perpendicularly to the target plane with an $f/8$ optics. The laser spot was measured to have a diameter of 60 μm FWHM at the best focus. The focal depth was estimated to be ± 300 μm. The interaction region was magnified and imaged out in 2ω light on the cathode of a 120 ps gate time Gated Optical Intensifier (GOI). A fraction of this light was split out and sent to a photomultiplier to detect the amplitude of the second-harmonic signal. The 2ω region was spectrally selected by 3 nm FWHM interference filters centred at 532 nm.

i) *Second-harmonic emission vs. target position.* – The graph of fig. 2 shows second-harmonic power as a function of target position with respect to the laser beam waist for three different laser power levels. Measurements refer to a collection aperture $f/4$, twice the laser focusing aperture.

For 15 MW laser power, corresponding to an intensity at the beam waist of $5 \cdot 10^{11}$ W cm^{-2}, no dependence of the detected radiation on target position was found within the explored range. On the contrary, an incident laser power of 170 MW resulted in a strong dependence of 2ω emission on target position with a maximum at approximately + 600 μm from the nominal position of the laser beam waist. This behaviour was also observed for laser power of 800 MW, where the maximum emission was an order of magnitude higher than in the case of 170 MW laser power. Speculation on the shift of the maximum 2ω emission from the nominal focus requires a discussion on the methods used to determine the position of the focus itself. However, this analysis is not relevant to the aim of this letter and is reported elsewhere [12].

Actually, signals detected at marginal target positions (typically at distances greater than 1.5 mm from the position of maximum 2ω emission), as well as the whole curve at the lowest laser power level, have to be attributed to bremsstrahlung radiation in the frequency range allowed by the narrow-band filter rather than to second-harmonic generation. Such a

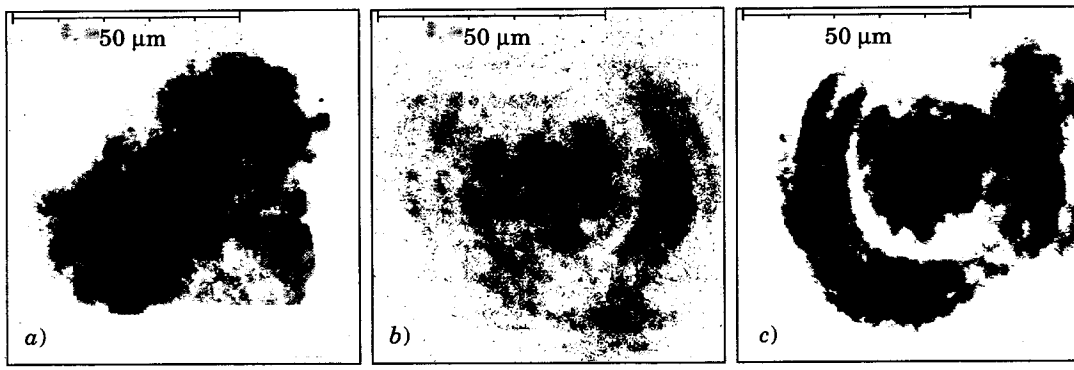

Fig. 4. – Gated Optical Intensifier images of the 2ω sources in the plasma. Gate time: 120 ps. Target position: *a*) – 600 μm, *b*) and *c*) + 400 μm (see also arrows in fig. 2).

conclusion was supported by the comparison of these measurements with test measurements performed by tilting the interference filter in a way that the spectral region allowed by the filter was shifted by the amount required to exclude second-harmonic light from the detected spectral window.

The most evident feature of the experimental data shown in fig. 2 is that the 2ω emission jumps up over bremsstrahlung by up to three orders of magnitude for relatively modest changes in experimental conditions. In addition, an increase in the level of 2ω emission up to two orders of magnitude is apparent for target displacements as small as 250 μm. This value is definitely smaller than the overall depth of focus of our focusing optics which was measured to be 600 μm. Therefore it is evident that some mechanism takes place which strongly modifies the laser intensity distribution generated by the focusing optics. This assumption is consistent with the dependence of 2ω emission on the incident laser power.

ii) *Second-harmonic emission vs. laser power on target.* – Figure 3 shows a plot of second-harmonic emission as a function of laser power in a range from 10 MW to 1 GW with the target at the position of maximum emission and, for comparison, at a marginal position.

With target close to the position of maximum 2ω and in the range of laser power P_ω between 0.1 and 1 GW, the second-harmonic power $P_{2\omega}$ scales approximately as the third power of P_ω. On the other hand, a sub-linear scaling of $P_{2\omega}$ is observable for target in the same position but $P_\omega < 0.1$ GW as well as for target at marginal position. As stated above, most of the light collected at marginal target positions is due to bremsstrahlung radiation. This fact can explain the weak dependence of this curve on incident laser power. On the contrary, the more than quadratic scaling of $P_{2\omega}$ with the target in the position of maximum conversion efficiency can only be explained if extra processes are included which can «boost» the non-linear second-harmonic conversion efficiency.

iii) *Time-resolved images of 2ω sources.* – Figure 4 shows three representative images of the sources of 2ω light into the plasma, as taken by the GOI device. The 120 ps gate time of the optical intensifier was located approximately at the peak of the laser pulse. The incident laser power was 800 MW and the target was 1 μm thick. Picture 4*a*) was obtained with target in position – 600 μm, which corresponds to a moderate 2ω production. The particular shape of this image, namely two main sources located at the ends of an inclined bar, was reproducible shot by shot. Pictures 4*b*) and *c*) were obtained with target in position + 400 μm, where 2ω emission was about 500 times higher than in the position of picture 4*a*). At + 400 μm the

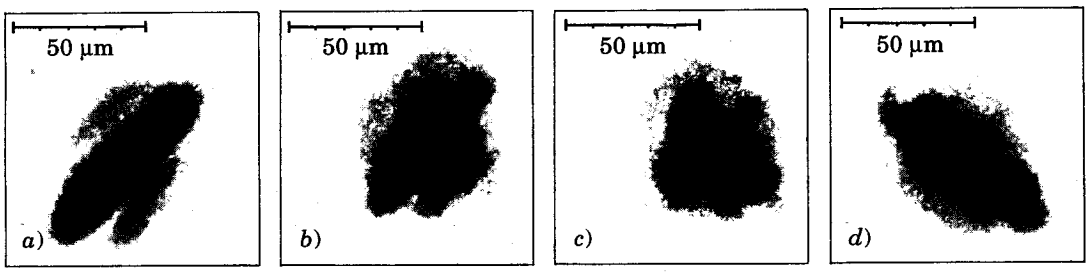

Fig. 5. – Equivalent plane images of the IR laser focal spot taken at different planes whose equivalent locations are *a*) −400 μm, *b*) −200 μm, *c*) 0 μm, *d*) 200 μm.

2ω images were not reproducible shot by shot. However, they always showed several small spots in the centre (typically ≈ 5 μm size) surrounded by ring structures of lower intensity. It is interesting to compare the pictures of fig. 4 with the IR images of the laser spot obtained at different planes close to the waist with the method of the equivalent plane monitor. An $f/100$ lens was used to this purpose. A series of those images is shown in fig. 5, where the equivalent positions of the respective planes are reported (as referred to the focal region of the $f/8$ lens focusing on the target). The images of fig. 5 clearly indicate that the laser beam is affected by astigmatism. No structures were evidenced with a size comparable with those observed in 2ω sources.

Comparison of picture *a*) in fig. 4 with the focal scan on fig. 5 evidences that, in condition of moderate second-harmonic generation, the structure of the 2ω source is imprinted by the astigmatism of the laser beam. The splitting of the elongated spot into two main 2ω sources could be attributed to the occurrence of some filamentation instability. However, the reproducibility shot by shot of the 2ω images in those conditions confirms that the original intensity distribution in the laser beam dominates in the creation of gradients. In conditions of high second-harmonic generation a completely different behaviour was observed, as shown in pictures *b*) and *c*) of fig. 4. In this case, no memory of the original laser spot structure is observable any more in the 2ω images and these latter are variable shot by shot, thus indicating that the instability dominates the interaction. Also the size of the intense small spots is comparable with the filament cross-section expected for the maximum growth of filamentation instability, as shortly pointed out below.

We know from previous measurements [10, 13] that at the peak of the laser pulse, with 1 μm formvar target in the best focus, the maximum density in our plasma is about a quarter of the critical density and the electron temperature is about 500 eV. From the ordinary steady-state theory of filamentation [14], ponderomotive filamentation is dominant for small structures and the optimum growth wavelength (twice the filament diameter) is $\lambda^{\mathrm{P}}_{\max} \approx 14$ μm at $n_c/4$. This value is consistent with the observed size of the intense 2ω spots showed in fig. 4*b*) and *c*). Also the growth length for modulation of that scale, calculated from theory [14], is consistent with the measured scalelength of the plasma density at $n_c/4$, about 30 μm [13]. At the same time we observed an effect on a larger scale, namely a whole-beam self-focusing which reduced the focal spot from 60 μm to (20 ÷ 30) μm size as shown in fig. 4*b*) and *c*). Following the ordinary theory this effect has to be of thermal origin.

Recently, a new model using Fokker-Planck transport calculations [15, 16] showed that in many experimental cases thermal filamentation can prevail over ponderomotive filamentation also for small modulations. Theory of ref. [15] gives for optimum growth wavelength and related growth length, due to thermal mechanism, the estimates $\lambda^{\mathrm{T}}_{\max} \approx 13$ μm and $(K^{\mathrm{T}}_{\max})^{-1} \approx$ ≈ 31 μm, respectively. They are also in agreement with our experimental results. It is relevant

that in the framework of this latter theory, both small-scale and whole-beam effects we have observed are explainable coherently in terms of thermal filamentation. The weak interference rings surrounding the central spots are likely due to second-harmonic sources located out of focus.

In conclusion, we obtained evidence of transition from a laser-plasma interaction regime dominated by the original beam profile to a regime where the filamentation instability grows up its own structures. The transition was observed as a function of two independent parameters: target position and laser power on target. In both cases we had indirect evidence of this transition by the dramatic increase of second-harmonic emission. In the first case (variation of target position) we had also a direct evidence by means of 2D time-resolved imaging. The position of the exploding foil determines the geometry of the interaction, *i.e.* the spatial relation between the waist of the focused beam and the plasma density profile, but slightly affects plasma density and temperature thanks to the large focal depth.

* * *

Authors are grateful to the Plasma Physics Group of Imperial College, for the loan of the GOI device used in this experiment. Useful discussions and comments to this work are due to L. NOCERA, E. SCHIFANO, D. BATANI and F. BIANCONI. One of us (ID) gratefully acknowledges the International Centre for Theoretical Physics, Trieste, Italy, for its research grant. The research programme on laser-plasma interaction is fully supported by Consiglio Nazionale delle Ricerche, Italy.

REFERENCES

[1] KRUER W. L., *Phys. Fluids B*, **3** (1991) 2356.
[2] WILLI O., AFSHAR-RAD T., COE S. and GIULIETTI A., *Phys. Fluids B*, **2** (1990) 1318.
[3] AFSHAR-RAD T., GIZZI L. A., DESSELBERGER M., KATTAK F., WILLI O. and GIULIETTI A., *Phys. Rev. Lett.*, **68** (1992) 942.
[4] GREK B., MARTIN F., JOHNSTON T. W., PEPIN H., MITCHEL G. and RHEAULT F., *Phys. Rev. Lett.*, **41** (1978) 1811.
[5] WILLI O. and RUMSBY P. T., *Opt. Commun.*, **37** (1981) 45.
[6] YOUNG P. E., *Phys. Fluids B*, **3** (1991) 2331.
[7] STAMPER J. A., LEHMBERG R. H., SCHMITT A., HERBST M. J., YOUNG F. C., GARDNER J. H. and OBENSCHAIN S. P., *Phys. Fluids*, **28** (1985) 2563.
[8] BATANI D., BIANCONI F., GIULIETTI A., GIULIETTI D. and NOCERA L., *Opt. Commun.*, **70** (1989) 38.
[9] YOUNG P. E., BALDIS H. A., JOHNSTON T. W., KRUER W. L. and ESTABROOK K. G., *Phys. Rev. Lett.*, **63** (1989) 2812.
[10] GIULIETTI A., GIULIETTI D., BATANI D., BIANCALANA V., GIZZI L., NOCERA L. and SCHIFANO E., *Phys. Rev. Lett.*, **63** (1989) 524.
[11] GIULIETTI A., GIULIETTI D., NOCERA L., DEHA I., CHEN ZEZUN and BANFI G. P., *Laser Interaction and Related Plasma Phenomena*, Vol. 8 (Plenum Press, New York, N.Y.) 1988, p. 365.
[12] CHESSA P., Thesis, Department of Physics Library, University of Pisa (1991).
[13] GIULIETTI D., BIANCALANA V., BATANI D., GIULIETTI A., GIZZI L., NOCERA L. and SCHIFANO E., *Nuovo Cimento D*, **13** (1991) 845.
[14] SODHA M. S., GHATAK A. K. and TRIPATHI V. K., *Progress in Optics*, Vol. **13** (Academic Press, New York, N.Y.) 1976, p. 169.
[15] EPPERLEIN E. M., *Phys. Rev. Lett.*, **65** (1990) 2145.
[16] EPPERLEIN E. M., *Phys. Fluids B*, **3** (1991) 3082.